EUV Emission Spectra of Gd and Tb Ions

D. Kilbane[1, a)] and G. O'Sullivan[1]

School of Physics, University College Dublin, Belfield, Dublin 4, Ireland

(Dated: 27 October 2010)

Theoretical EUV emission spectra of gadolinium and terbium ions calculated with the Cowan suite of codes and the FAC relativistic code are presented. $4d-4f$ and $4p-4d$ transitions give rise to unresolved transition arrays in a range of ions. The effects of configuration interaction are investigated for transitions between singly excited configurations. Optimization of emission at 6.775 nm and 6.515 nm is achieved for Gd and Tb ions respectively by consideration of plasma effects. The resulting synthetic spectra are compared with experimental spectra recorded using the laser produced plasma technique.

PACS numbers: 32.30.Jc, 52.50.Dg

[a)]Electronic mail: deirdre.kilbane@ucd.ie

I. INTRODUCTION

Research into powerful sources for extreme ultraviolet lithography (EUVL) has concentrated at the 13.5 nm wavelength due to the high reflectivity of molybdenum/silicon mirrors at this wavelength[1–4]. Currently both laser produced plasmas (LPPs) and discharge plasmas of Sn and Xe targets are being used as the EUV source. The atomic processes in Xe and Sn have been successfully modeled previously[1,4–8], with $4d-4f$ and $4p-4d$ transitions identified as giving rise to large emission at 13.5 nm in Sn^{8+} - Sn^{13+} ions and $4d-5p$ transitions in Xe^{10+}. Despite huge theoretical efforts employing radiation hydrodynamic codes[9–11], the required 200 W output in a 2% bandwidth and high conversion efficiency (CE) still remains unattainable. It has been proposed that a higher CE can be achieved for EUV sources by using a Nd:YAG laser to pump the source prior to irradiation from a CO_2 laser[11].

Future sources for EUVL will endeavour to operate at shorter wavelengths, for example $\lambda/2 = 6.75$ nm, using the same instrumental arrangement with the replacement of the Mo /Si mirrors with optics suitable for 6.75 nm. Gadolinium and terbium ions were shown to be strong emitters at this wavelength, due mainly to the presence of unresolved transition arrays (UTAs) in the emission spectra[12]. Extreme UV spectra of Gd and Tb ions excited in laser-produced plasmas and vacuum spark sources were recorded in the $40-120\mathring{A}$ region and investigated on the basis of Hartree-Fock calculations using the Cowan code[13,14]. Maxima found at 6.775 nm and 6.515 nm (for Gd and Tb ions respectively), were attributed to $4d-4f$ and $4p-4d$ transitions in ions with $4p^6 4d^N$ ($N = 8$ - 10) and $4d^{10}4f^M$ ($M = 1$ - 2) ground configurations. This work investigates further the conditions necessary to optimize the emission from these sources, in particular to account for plasma effects.

This article is organized as follows: in sec II A and sec II B we present theoretical calculations of energy levels and line strengths using the FAC code[15]. Influence of configuration interaction on line strengths is discussed in sec II B. Also the contribution from $4d-4f$ and $4p-4d$ transitions are displayed in this section. Plasma effects are considered in sec III: ionic populations calculated from a collisional radiative (CR) model are presented in sec III A while temperature dependent spectra assuming a Boltzmann distribution of excited states are shown in sec III B. In sec IV theoretical spectra are compared with experimental spectra. Finally the article is concluded in sec V.

II. DETAILED ATOMIC CALCULATIONS

Configuration interaction calculations were performed using the Hartree-Fock with relativistic and correlation corrections mode of the Cowan suite of atomic codes[14] for the ions and basis sets defined in table I. In general it is necessary to compensate for the effect of missing configurations by varying the Slater parameters F^k, G^k and the configuration interaction parameter R^k from their *ab initio* values, while retaining the spin-orbit parameter value. Extensive investigations of experimental spectra[13,16,17] of these ions, which led to spectroscopic detailing of lines and energy levels, provided suitable scaling parameters for this study. For Ag I and Pd I like ions the Slater Condon parameters were reduced by 15% while the spin orbit integrals were left unchanged as in the earlier work[16,17]. For more highly charged ions, the electrostatic and configuration interaction parameters were reduced by 10% as suggested by Churilov *et al*[13]. In addition calculations were performed using the FAC code[15] which uses a fully relativistic approach based on the Dirac equation, thus allowing its application to ions with large values of nuclear charge. Ground state configurations in open f subshell ions were assigned on the basis of the lowest average energy provided by the Cowan code calculations.

A. Distribution of Energy Levels

The energy levels calculated using the FAC code are presented for Gd ions in Fig. 1 which shows the spread in excited levels. A similar spread in excited states is observed for Tb ions. The distribution of energy levels remains largely unchanged for both elements when configuration interaction is included/excluded. Transitions between singly excited states in addition to resonance transitions have been included in the following calculations. From the distribution of energy levels it can be inferred that emission could be enhanced by transitions between singly excited states with $\Delta n = 0$, $n > 4$ or $\Delta n > 0$ as these can be populated at high plasma temperatures. In the present case however any contribution lies outside the wavelength range of interest as will be shown in sec II B. Also indicated in Fig. 1 are the number of states for each ion which will be considered further in sec III A.

B. Distribution of Line Strengths

It is well known that configuration interaction (CI) redistributes line strengths and positions providing a more accurate description of experimental spectra[14]. CI calculations on Sn demonstrated a shift of the $4d-4f$ and $4p-4d$ transitions to shorter wavelength and a narrowing of the spectral width[18]. A detailed study of the effect of CI on Xe ions showed the large increase in the number of transitions when CI is included[8]. The effect of configuration interaction on line strengths was investigated for a range of ions, Gd^{20+} - Gd^{25+} and Tb^{21+} - Tb^{26+}, and is presented in Fig. 2 and Fig. 3 respectively. All detailed spectra in this work are convolved with a Gaussian profile of width 0.2 eV to simulate experimental conditions. CI leads to an increase in maximum line strength and a narrowing of the peak for all ions considered. Also the position of the peak is seen to vary only slightly by ≤ 0.2 nm. This centering of the peak implies that strong emission should be achievable over a wide range of plasma conditions which will be discussed further in sec III.

Also shown in Fig. 2 and Fig. 3 are the contributions from $4d-4f$ and $4p-4d$ transitions. In all ion stages these transitions give rise to the strongest peak, with the $\Delta n > 0$ transitions not influencing the peak emission greatly. Previous studies on Sn and Xe reported that the resonant transition contribution to emission is greatly enhanced by the presence of satellite lines[8,19,20]. The inclusion of doubly excited states in Gd and Tb will be considered in a future work.

In the absence of experimentally determined lines and levels such as are available for Sn[6,21], the Cowan code spectra were used to reproduce previously determined experimental spectroscopic lines and energy positions accurately[16,17]. The corresponding FAC spectra were always found to be at slightly shorter wavelengths in this work. Hence a wavelength correction was subsequently applied to the FAC spectrum calculated for each ion, which was individually shifted by ≤ 0.2 nm (shifts decreased from 0.2 nm in Gd XVIII to 0.095 nm in Gd XXVIII). With these wavelength corrections it was seen that the Cowan and FAC spectra were essentially the same. The resulting shifted line strength spectra are presented in Fig. 4 and Fig. 5 for the total range of ions used in this study, namely, Gd^{16+} - Gd^{27+} and Tb^{17+} - Tb^{28+}. Purely from consideration of these line strengths, experimental EUV maxima recorded at 6.775 nm and 6.615 nm are predicted to arise from UTAs in Gd^{20+} - Gd^{24+} and Tb^{21+} - Tb^{25+} respectively. Notice the contribution from $\Delta n > 0$ at longer wavelengths as

was observed previously for Xe and Sn ions[7,19].

III. PLASMA EFFECTS

A. Collisional Radiative Model

Detailed modeling of the EUV emission of a LPP, which requires knowledge of the populations of excited states at all temperatures, is computationally very intensive. The CR model of Colombant and Tonon has been widely used as a first approximation to calculate ionic populations as a function of electron density (N_e) and average electron temperature (T_e)[7,9,12,22]. Collisional ionization, radiative recombination and three-body recombination are included in this model using semi-empirical formulae. Ionic populations and average ionization $< Z^* >$ are presented for Gd in Fig. 6, at an electron density of $N_e = 10^{21}$ cm^{-3}. Results for Tb closely resemble those of Gd due to their similar nuclear charge.

For a laser power density of $(5-8) \times 10^{11}$ W cm^{-2}, as used in earlier experiments[13], this model predicts an average electron temperature of $135 \leq T_e \leq 180$ eV. Ions in this region have open $4d$ subshells only whereas a lowering of the laser power density would lead to the opening of the $4f$ subshell. This gives rise to enormous numbers of transitions due to the large number of excited states with energies very close to the ground state[12,23,24]. The $4-4$ band of transitions for these ions could overlap with the higher ion stages and give rise to further enhancement of the EUV emission at 6.675 nm[13]. As shown in Fig. 1 there is a huge increase in the number of states for Gd XVII resulting from the opening of the $4f$ subshell. A future systematic investigation would reveal the extent of the contribution of these ions at lower temperatures.

B. LTE Assumption

In addition to resonant lines, transitions between singly excited states are also considered in this work. Since radiative transitions with different initial states are involved, the line strengths must be suitably weighted. At electron densities $N_e \geq 10^{20}$ cm^{-3} the populations of excited states within each ion stage can be assumed to be in Local Thermodynamic Equilibrium (LTE) and can be described by a Boltzmann distribution[25]. Fig. 7 and Fig. 8 show the resulting intensity, weighted by ionic populations taken from Fig. 6, for a range

of temperatures. For each ion stage from XIX - XXV, a temperature was chosen where the peak ionic population for that ion was observed.

IV. EXPERIMENTAL COMPARISON

The experimental EUV spectra of Gd and Tb ions excited in a LPP were recorded previously[13]. The extremely sharp peaks with maxima at 67.75$\mathring{A}$ for Gd ions and 65.15$\mathring{A}$ for Tb ions were attributed to the overlapped $4-4$ transitions in the ions with $4p^6 4d^N$ $(N = 8-10)$ and $4d^{10}4f^M$ $(M = 1-2)$ ground configurations. However plasma effects were not considered in this earlier work. Assuming CR equilibrium for ionic populations and LTE for level populations in the plasma, it is estimated that a plasma electron temperature of $T_e = 144$ eV for Gd, and $T_e = 152$ eV for Tb, account for the experimental emission peaks which result mainly from Gd^{20+} - Gd^{22+} and Tb^{20+} - Tb^{23+}. Fig. 9 shows the comparison between the earlier experimental spectra[13] and the current theoretical spectra. Overall good agreement can be seen for the shape and position of the emission peaks. Discrepancies can be attributed to the exclusion of doubly excited states, which give rise to satellite lines, that increased peak emission substantially in the case of Xe and Sn ions[4,8,19]. Also since the theoretical spectra are essentially snapshots of a single plasma temperature and the experimental spectra are time integrated over a range of plasma conditions, strong resonance lines from lower ion stages are also evident in the latter. For example the $4d^{10}\ ^1S_0 - 4d^9 4f\ ^1P_1$ lines of Gd XIX and Tb XX[16] are clearly visible in both experimental spectra. Even tiny populations of these ions will lead to relatively intense emission due to the small number of lines available in these spectra compared to those from open $4d^N$ ions.

V. CONCLUSION

EUV emission spectra resulting from $4d-4f$ and $4p-4d$ transitions in Gd and Tb ions have been presented. CR modeling of the hot dense plasma, accounting for the thermodynamic population of levels, allowed for the construction of temperature dependent spectra. UTAs centered at 6.775 nm in Gd and 6.515 nm in Tb, result in maximum emission under the following plasma conditions at $N_e = 10^{21}$ cm^{-3}: $T_e = 144$ eV and $T_e = 152$ eV for Gd and Tb ions respectively. Future investigations will concentrate on contributions from

doubly excited states, and the large number of transitions in lower ion stages. Both are expected to enhance peak emission while their complexity will smooth the overall profile. Consideration of self absorption, which is known to occur in LPPs at these power densities, will reduce the strongest lines most and hence lead to an overall smoother profile. This work could help to extend current nanolithography research to shorter wavelengths.

ACKNOWLEDGMENTS

This work was supported by Science Foundation Ireland under Principal Investigator research grant 07/IN.1/B1771. We wish to thank A. N. Ryabtsev for generously providing the experimental spectra.

REFERENCES

[1]S. S. Churilov, Y. N. Joshi, J. Reader, and R. R. Kildiyarova, Phys. Scr., **70**, 126 (2004).

[2]V. Bakshi, ed., *EUV Sources for Lithography* (SPIE, Bellingham, WA, 2005).

[3]G. O'Sullivan, A. Cummings, C. Z. Dong, P. Dunne, P. Hayden, O. Morris, E. Sokell, F. O'Reilly, M. G. Su, and J. White, J. Phys.: Conf. Ser., **163**, 012003 (2009).

[4]A. Sasaki, A. Sunahara, H. Furukawa, K. Nishihara, S. Fujioka, T. Nishikawa, F. Koike, H. Ohasni, and H. Tanuma, J. Appl. Phys., **107**, 113303 (2010).

[5]N. Böwering, M. Martins, W. N. Partlo, and I. V. Fomenkov, J. Appl. Phys., **95**, 16 (2004).

[6]S. S. Churilov and A. N. Ryabtsev, Phys. Scr., **73**, 614 (2006).

[7]M. Poirer, T. Blenski, F. de Gaufridy de Dortan, and F. Gilleron, J. Quant. Spectrosc. Radiat. Transfer, **99**, 482 (2006).

[8]F. de Gaufridy de Dortan, J. Phys. B: At. Mol. Opt. Phys., **40**, 599 (2007).

[9]A. Cummings, G. O'Sullivan, P. Dunne, E. Sokell, N. Murphy, J. White, K. Fahy, A. Fitzpatrick, L. Gaynor, P. Hayden, D. Kedzierski, D. Kilbane, M. Lysaght, L. McKinney, and P. Sheridan, J. Phys. D: Appl. Phys., **37**, 2376 (2004).

[10]A. Cummings, G. O'Sullivan, P. Dunne, E. Sokell, N. Murphy, and J. White, J. Phys. D: Appl. Phys., **38**, 604 (2005).

[11]K. Nishihara, A. Sunahara, A. Sasaki, M. Nunami, H. Tanuma, S. Fujioka, Y. Shimada, K. Fujima, H. Furukawa, T. Kato, F. Koike, R. More, M. Murakami, T. Nishikawa, V. Zhakhovskii, K. Gamata, A. Takata, H. Ueda, H. Nishimura, Y. Izawa, N. Miyanaga, and K. Mima, Phys. Plasmas, **15**, 056708 (2008).

[12]G. O'Sullivan, J. Phys. B: At. Mol. Opt. Phys., **16**, 3291 (1983).

[13]S. S. Churilov, R. R. Kilidiyarova, A. N. Ryabtsev, and S. V. Sadovsky, Phys. Scr., **80**, 045303 (2009).

[14]R. D. Cowan, *The Theory of Atomic Structure and Spectra* (University of California Press, Berkeley, CA, 1981).

[15]M. F. Gu, Astrophys. J., **582**, 1241 (2003).

[16]J. Sugar, V. Kaufman, and W. L. Rowan, J. Opt. Soc. Am. B, **10**, 799 (1993).

[17]J. Sugar, V. Kaufman, and W. L. Rowan, J. Opt. Soc. Am. B, **10**, 1321 (1993).

[18]W. Svendsen and G. O'Sullivan, Phys. Rev. A, **50**, 3710 (1994).

[19]F. Gilleron, M. Poirer, T. Blenski, M. Schmidt, and T. Ceccotti, J. Appl. Phys., **94**, 2086 (2003).

[20]A. Sasaki, A. Sunahara, K. Nishihara, T. Nishikawa, F. Koike, and H. Tanuma, J. Phys.: Conf. Ser., **163**, 012107 (2009).

[21]R. D'Arcy, H. Ohashi, S. Suda, H. Tanuma, S. Fujioka, H. Nishimura, K. Nishihara, C. Suzuki, T. Kato, F. Koike, A. O'Connor, and G. O'Sullivan, J. Phys. B: At. Mol. Opt. Phys., **42**, 165207 (2009).

[22]D. F. Colombant and G. F. Tonon, J. Appl. Phys., **44**, 3524 (1973).

[23]P. K. Carroll and G. O'Sullivan, Phys. Rev. A, **25**, 275 (1982).

[24]G. O'Sullivan, P. K. Carroll, P. Dunne, R. Faulkner, C. McGuinness, and N. Murphy, J. Phys. B: At. Mol. Opt. Phys., **32**, 1893 (1999).

[25]A. Sasaki, K. Nishihara, M. Murakami, F. Koike, T. Kagawa, T. Nishikawa, K. Fujima, T. Kawamura, and H. Furukawa, App. Phys Lett., **85**, 5857 (2004).

TABLE I. Singly excited configurations of Gd and Tb ions included in the calculations.

Gd XVII - Gd XVIII	Gd XIX	Gd XX - Gd XXVIII
Tb XVIII - Tb XIX	Tb XX	Tb XXI - Tb XXIX
$4p^6 4d^{10} 4f^M$	$4p^6 4d^{10}$	$4p^6 4d^N$
$4p^6 4d^9 4f^{M+1}$	$4p^6 4d^9 nl$	$4p^6 4d^{N-1} nl$
$4p^6 4d^9 4f^M nl$		$4p^5 4d^{N+1}$
$(n \leq 8, l \leq 3, M \leq 2)$	$(1 \leq N \leq 10)$	

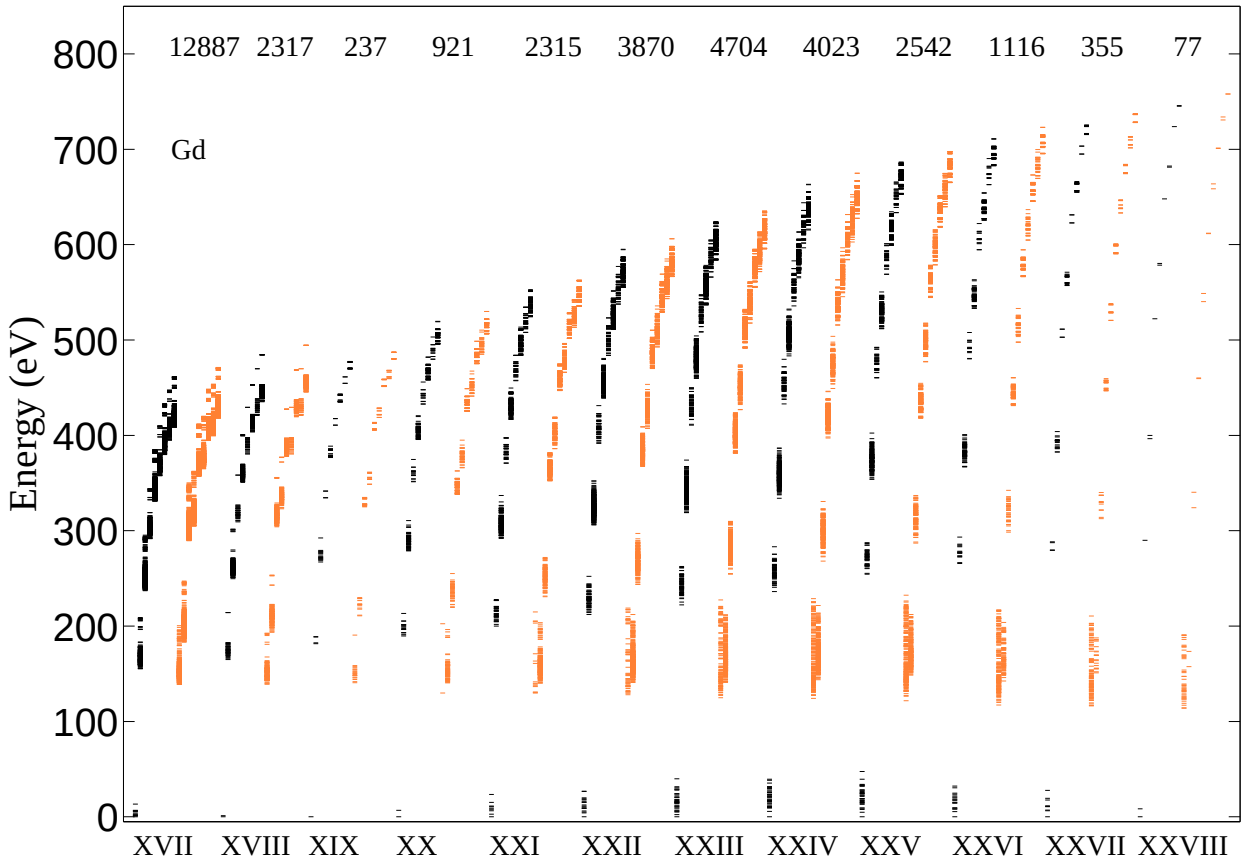

FIG. 1. (Color online) Energy levels of Gd^{16+} - Gd^{27+} computed with the FAC code including configuration interaction. Black and red lines denote different parity states. The numbers of states for each ion is shown at the top.

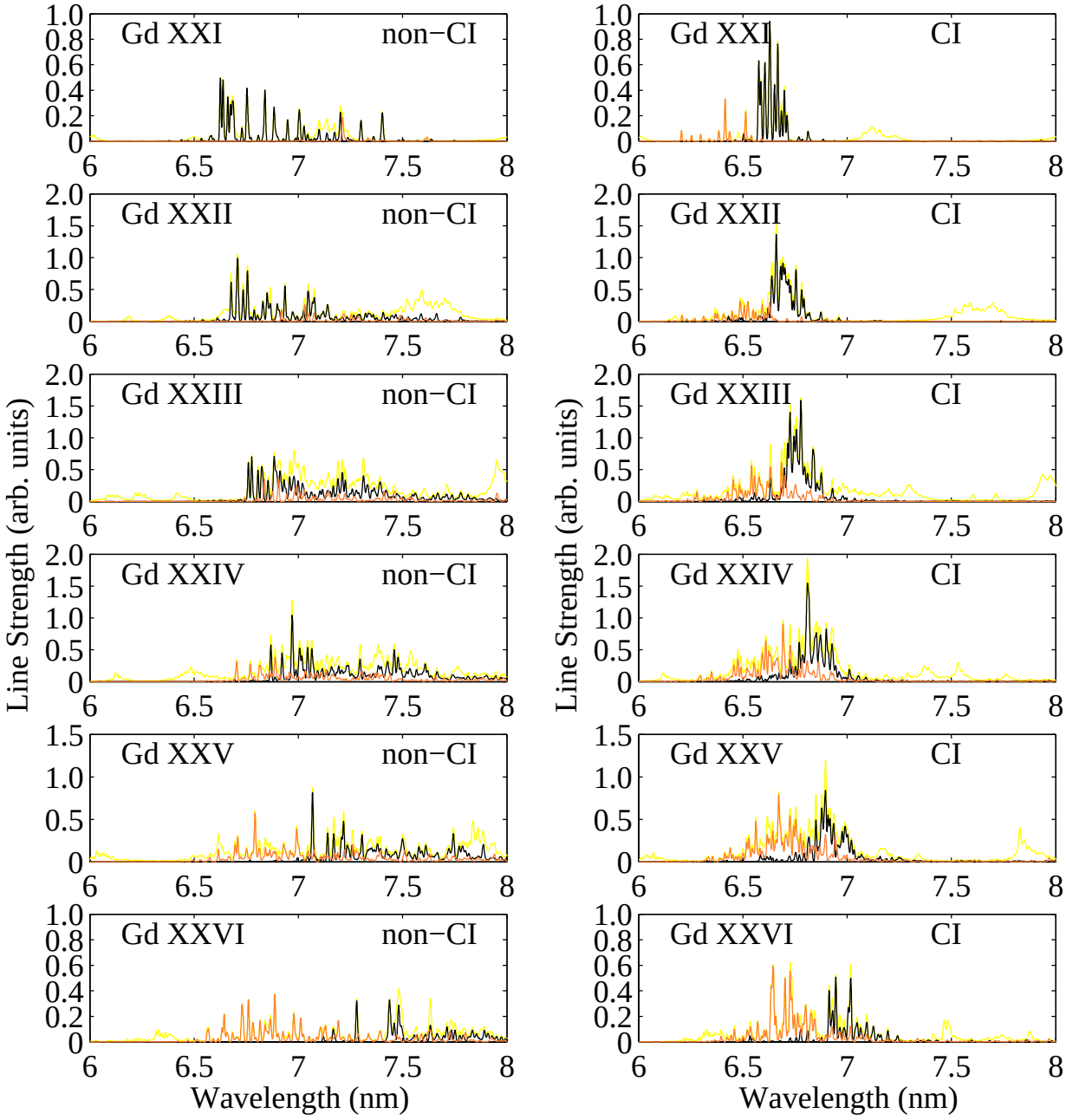

FIG. 2. (Color online) Gd^{20+} - Gd^{25+} spectra computed with the FAC code, excluding CI (left) and including CI (right). Blue denotes $4d - 4f$ transitions, red denotes $4p - 4d$ transitions and black denotes all transitions.

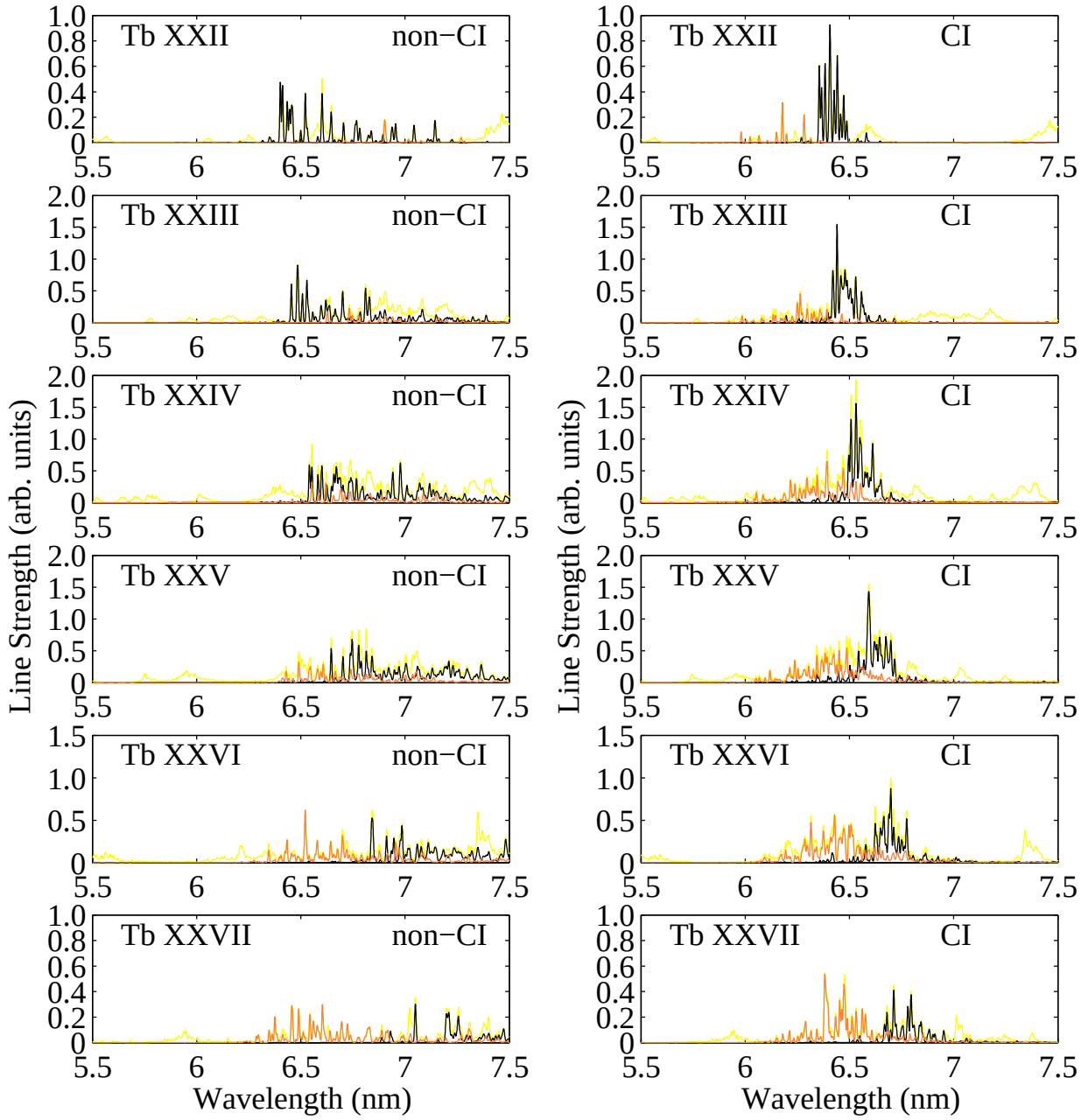

FIG. 3. (Color online) Tb^{21+} - Tb^{26+} spectra computed with the FAC code, excluding CI (left) and including CI (right). Blue denotes $4d - 4f$ transitions, red denotes $4p - 4d$ transitions and black denotes all transitions.

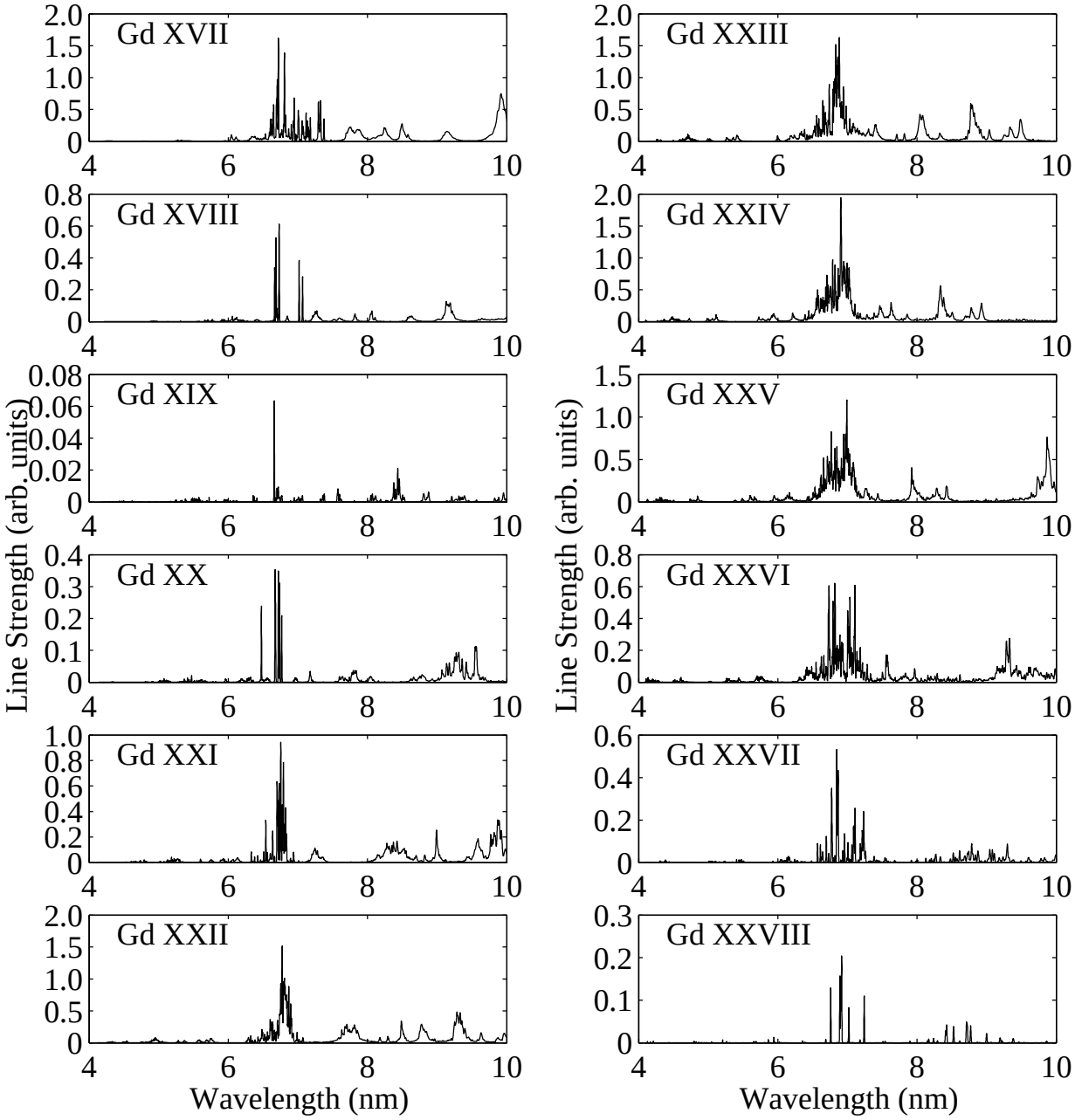

FIG. 4. Line Strength of Gd^{16+} - Gd^{27+} computed with the FAC code including the effects of CI.

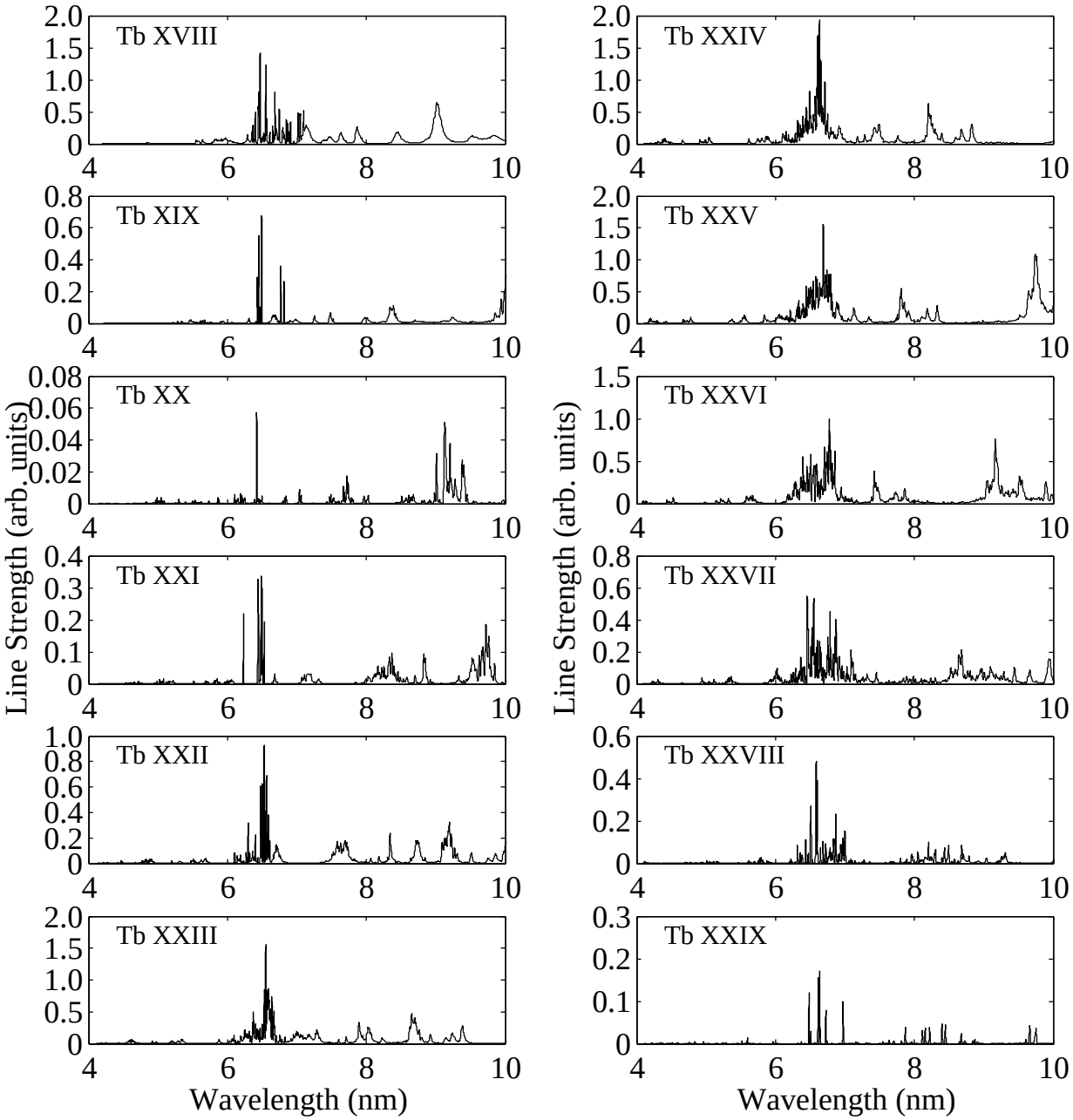

FIG. 5. Line Strength of Tb^{17+} - Tb^{28+} computed with the FAC code including the effects of CI.

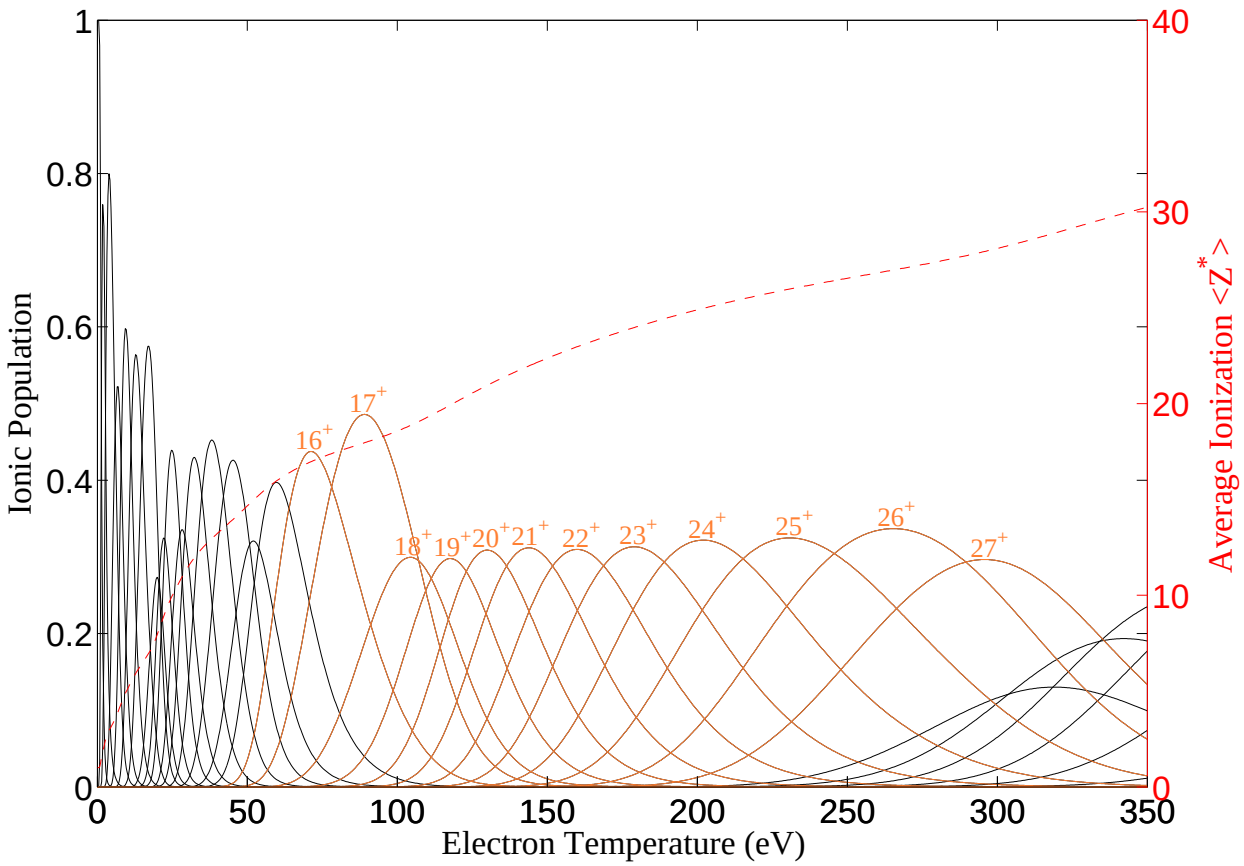

FIG. 6. (Color online) Ionic populations and average ionization of a Gd plasma as a function of T_e computed using the CR model. Ion stages considered in this work are shown in blue.

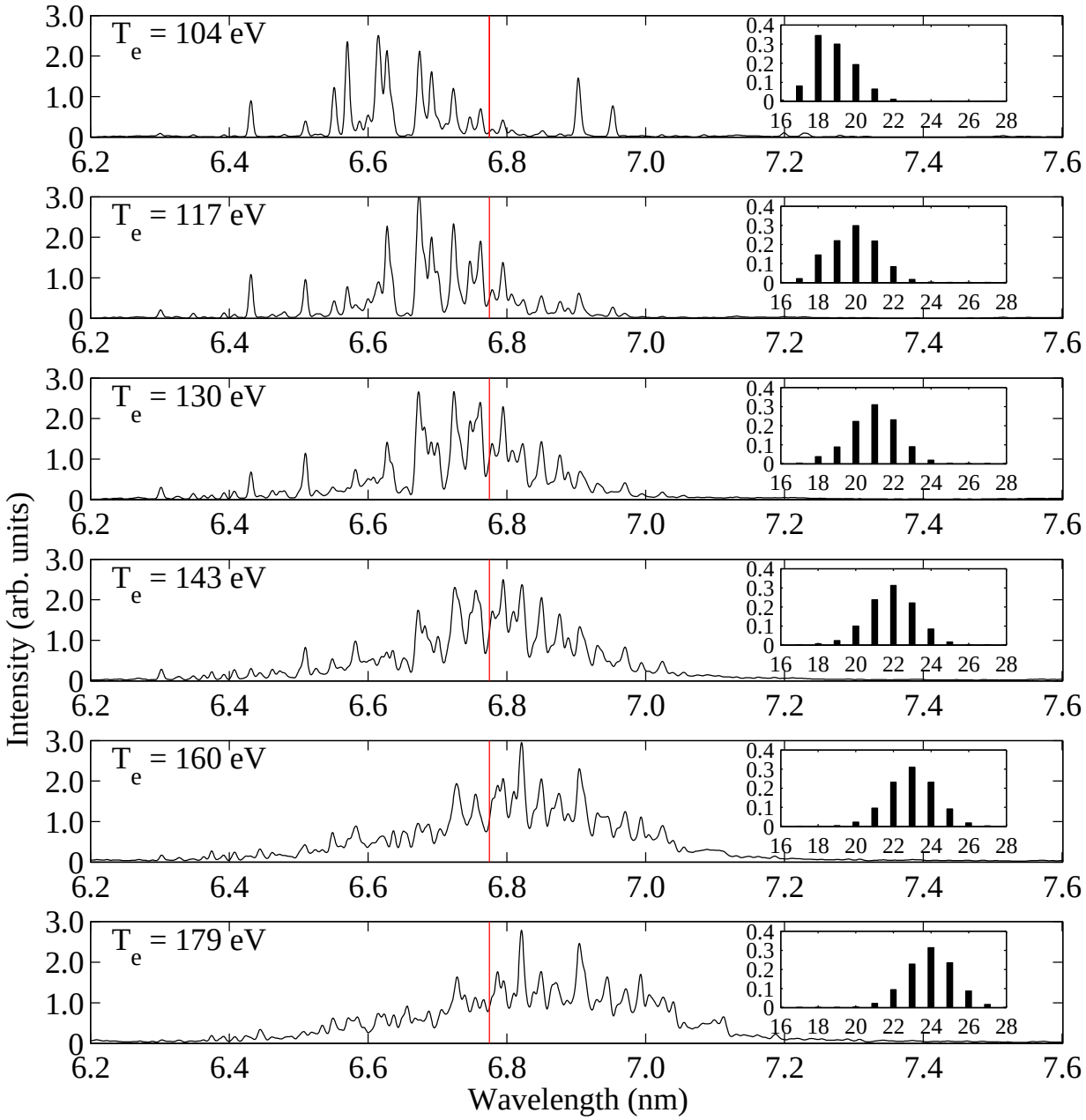

FIG. 7. (Color online) Intensity of Gd at various electron temperatures T_e in the plasma. The inset shows the ionic populations at each temperature.

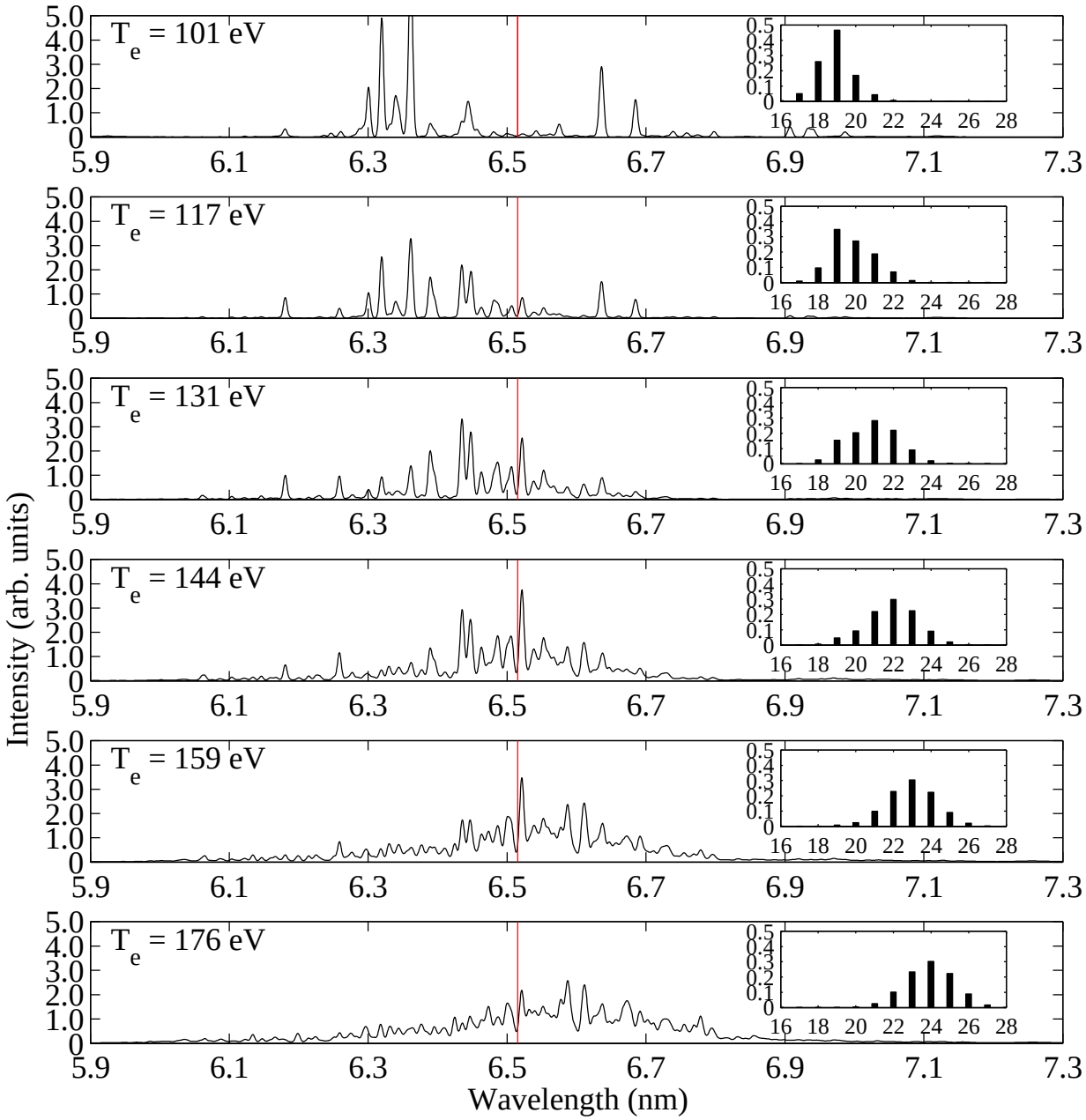

FIG. 8. (Color online) Intensity of Tb at various electron temperatures T_e in the plasma. The inset shows the ionic populations at each temperature.

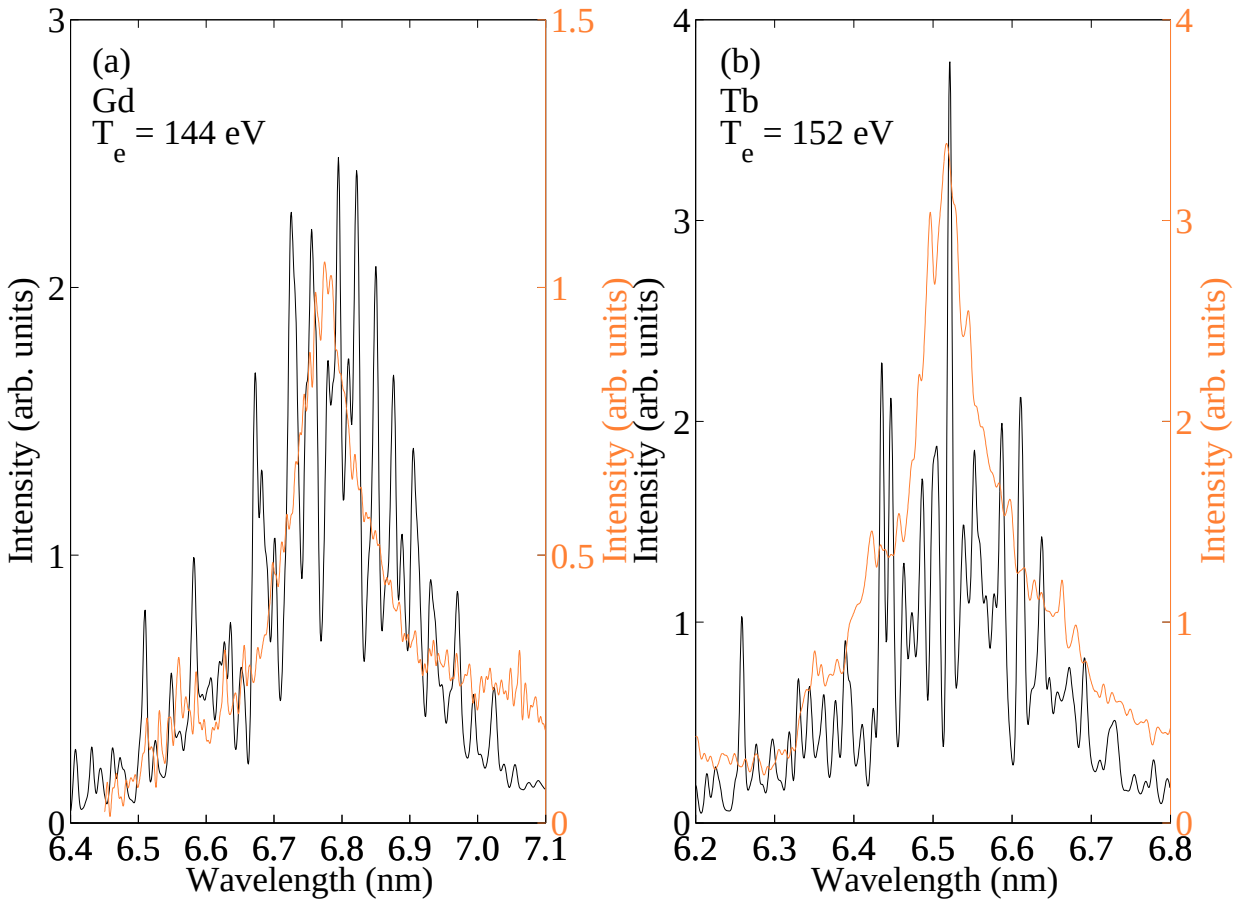

FIG. 9. (Color online) Current theoretical (black) and earlier experimental (red) spectra[13] of (a) Gd and (b) Tb.